

Kinetics of Hydrolytic Degradation of Poly(ethylene naphthalene-2,6-dicarboxylate)

H. Zhang and I. M. Ward*

IRC in Polymer Science & Technology, The University of Leeds,
Leeds LS2 9JT, United Kingdom

Received June 2, 1995; Revised Manuscript Received August 14, 1995*

ABSTRACT: The hydrolytic stability of both isotropic and oriented semicrystalline poly(ethylene naphthalene-2,6-dicarboxylate), PEN, films in saturated steam at temperatures 120–160 °C is reported. The kinetics of hydrolytic degradation of the semicrystalline PEN samples, together with semicrystalline PET, was studied by determining the rates of formation of carboxyl ends using infrared spectroscopy. Water vapor diffusion rates and water vapor solubilities of PEN and PET samples at various temperatures were also measured. The water vapor diffusion rates of PEN were found to be 2–3 times slower than those of PET. However, the water vapor diffusion rates of both PEN and PET were 3–4 orders of magnitude greater than their hydrolytic degradation rates. The hydrolysis in all the cases is therefore believed to be a chemical reaction rate controlled process. PEN, especially when oriented, showed better hydrolytic stability than PET. A half-order autocatalytic reaction mechanism with the carboxyl end groups acting as the catalyst gave the best explanation of the experimentally measured degradation rates, and from this analysis hydrolytic degradation rate constants were derived for PEN and PET.

Introduction

Poly(ethylene naphthalene-2,6-dicarboxylate) (PEN) is attracting increasing attention and larger scale commercialization, promoted by a major facility for producing dimethyl naphthalene-2,6-dicarboxylate, is underway. PEN is very similar to poly(ethylene terephthalate) (PET) in its structure but contains naphthalene rings which produce much stiffer molecular chains than those of PET, which contains benzene rings.^{1–3} The rigidity of the polymer backbone elevates the glass transition temperature (120 °C compared with 70 °C), enhances mechanical properties such as tensile modulus and creep resistance, and lowers shrinkage.⁴ Excellent barrier properties with respect to oxygen and carbon dioxide have also been reported.⁵

As a polyester, however, PEN hydrolyzes like PET under conditions of high humidity, where the ester functionality is vulnerable. The hydrolytic degradation of PET has been studied extensively.^{6–15} A systematic study by Ravens and co-workers in the early 1960s of the hydrolytic degradation of PET revealed that the hydrolytic scission of polyester chains above their glass transition temperature was an autocatalytic reaction and the process was chemical reaction rate controlled.^{6–8} Zimmerman and co-workers studied the hydrolytic degradation rate of samples of PET which had been polymerized using various catalysts.⁹ More recently, the effects of molecular weight and crystallinity on the hydrolytic degradation rate have been reported.^{11–14}

The hydrolytic degradation of polyesters involves the chemical scission of an ester linkage by a water molecule. Each chain scission uses up one water molecule and creates one carboxyl end group. Hence, the reaction can be followed by measuring the number of carboxyl ends present after various hydrolytic degradation times. In this study, the hydrolytic degradation of PEN at temperatures above its glass transition was investigated by using infrared end-group analysis. In particular, the hydrolytic degradation rates of PEN and PET were compared. The contribution of water sorption and

diffusion to the hydrolytic degradation of the materials is discussed.

Experimental Section

Sample Preparation. Amorphous and isotropic PEN and PET cast films (0.2–0.5 mm in thickness) were kindly supplied by Amoco Chemicals (Europe) SA, Geneva, Switzerland, and ICI Films, Middlesbrough, UK. Oriented PEN samples were obtained by uniaxial drawing of the films at 137 °C, with a draw ratio of 3.8 and a drawing speed of 6 mm/s. The draw ratio of 3.8 was slightly higher than the natural draw ratio for the sample at the temperature and draw speed used to achieve uniform drawing.

The drawn and the two isotropic films were annealed at 200 °C for 20 min under slight tension (in order to keep the film flat). X-ray photographs (Figure 1) showed that all the annealed samples were highly crystalline. Their crystallinity was calculated from their densities, measured in a density column (potassium iodide solution), using the equation

$$w_c = \frac{\rho_c(\rho - \rho_a)}{\rho(\rho_c - \rho_a)} \quad (1)$$

where ρ is the measured density value in g/cm³, and ρ_a and ρ_c are the amorphous and crystalline densities, respectively, taken from the literature. They are, for PET, $\rho_a = 1.333$ and $\rho_c = 1.515$ ¹⁶ and, for PEN, $\rho_a = 1.325$ and $\rho_c = 1.4007$.³ The results are summarized in Table 1.

Hydrolysis. All the samples were hydrolyzed for various times in saturated steam at 120, 140, and 160 °C. For the hydrolytic degradation at 120 °C, a commercial portable autoclave was used. For higher temperatures, a modified chemical reactor was used. Both the autoclave and the reactor had valves fitted allowing for the discharge of air trapped in the container and in the distilled water used for hydrolysis. In this way an exact temperature–pressure correlation was established according to steam tables.¹⁷

Infrared End Group Analysis. Methods reported in the literature for quantifying the extent of hydrolytic degradation as a function of reaction time include solution viscometry, end group analysis by titration or infrared (IR) spectroscopy, and gel permeation chromatography. In this study, infrared (IR) spectroscopic analysis of the film samples was used to measure the change in the number of end groups of PEN and of PET, a similar method to that used in the early work by Ward.¹⁸ The details of this analysis are reported elsewhere.¹⁹ A brief account is given here.

* Abstract published in *Advance ACS Abstracts*, October 15, 1995.

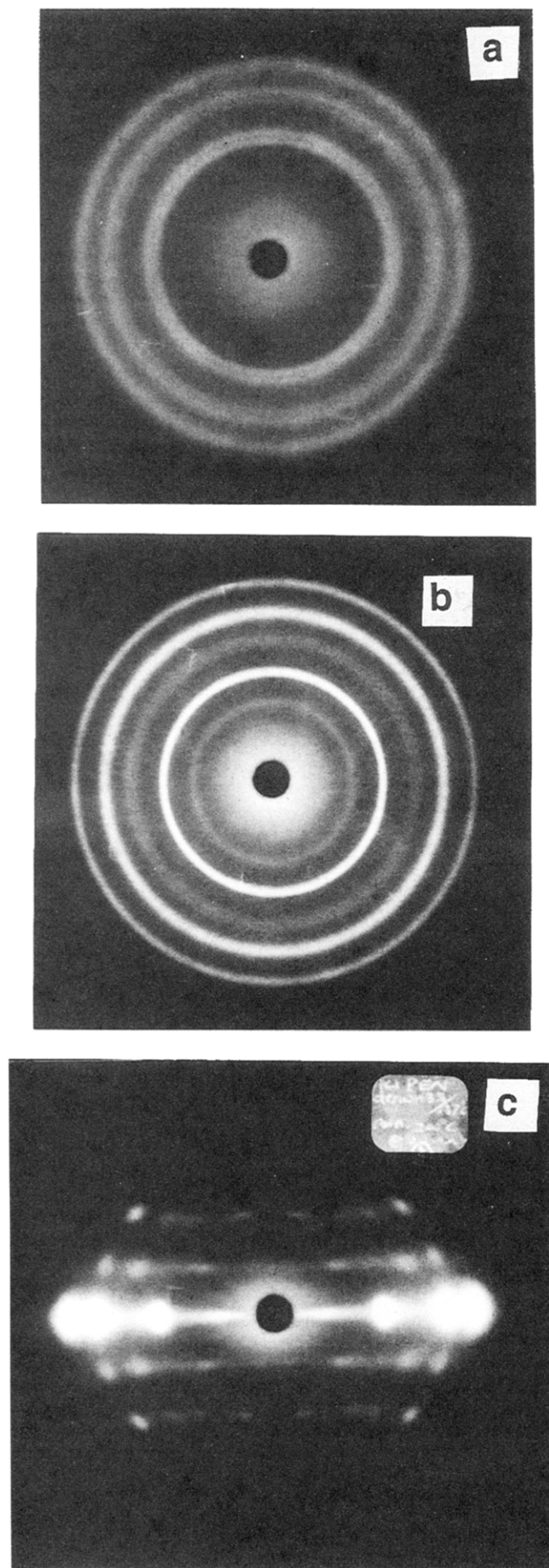


Figure 1. Wide-angle X-ray diffraction patterns of (a) annealed PET film, (b) annealed PEN film, and (c) uniaxially drawn and annealed PEN film. The draw direction of the PEN film is perpendicular to the incident X-ray beam.

Table 1. Molecular Weight, Density and Crystallinity of the Polyester Samples Used in This Study

sample	number average molecular weight ^a	density/ g cm ⁻³	crystallinity/ wt %
PET annealed	14 400	1.386	32
PEN annealed	13 400	1.349	33
PEN drawn and annealed	14 900	1.352	37

^a The values are based on the FT-IR end-group analysis.

The method involves a reference film, modified by deuteration, which quantitatively replaces the end-group protons with deuterons without affecting the protons in the main chain. The deuterated sample defines the background absorption spectrum for effectively zero end group content. Subtraction of this reference spectrum from the sample spectrum yields solely the absorption spectra of the end groups of the sample.

Provided there is no chain branching in the material, each molecule of both PET and PEN has two end groups, each of which may be a hydroxyl end, OH, or a carboxyl end, COOH. The end group concentrations, [OH] and [COOH], can be calculated from their IR absorption based on the Beer-Lambert law. A simple conversion gives

$$[\text{COOH}] = \frac{10^3}{\rho \epsilon_{\text{COOH}}} A_{\text{COOH}} \quad \text{and} \quad [\text{OH}] = \frac{10^3}{\rho \epsilon_{\text{OH}}} A_{\text{OH}} \quad (2)$$

where [COOH] and [OH] are the concentrations of the carboxyl and hydroxyl groups, respectively, in mole/10⁶ g equiv; ρ is the sample density in g/cm³; l is the film thickness in cm; A_{COOH} and A_{OH} are the absorbance of COOH and OH, respectively; and ϵ_{COOH} and ϵ_{OH} are the IR extinction coefficients of COOH and OH, respectively, in liter L mol⁻¹ cm⁻¹.

Values of the ϵ_{COOH} and ϵ_{OH} were calibrated using a series of PET and PEN samples with different molecular weights as measured by solution viscometry. Using the integral IR absorbance of OH stretching vibration in the carboxyl end groups and hydroxyl end groups, the corresponding IR extinction coefficients were obtained as

$$\frac{1}{\epsilon_{\text{COOH}}} = (4.8 \pm 0.4) \times 10^{-5} \quad \text{and} \quad \frac{1}{\epsilon_{\text{OH}}} = (9.2 \pm 0.4) \times 10^{-5} \quad (3)$$

in L mol⁻¹ cm⁻¹ for both PET and PEN samples.

The number average molecular weight, M_n , is

$$M_n = \frac{2 \times 10^6}{[\text{COOH}] + [\text{OH}]} \quad (4)$$

The FT-IR spectra were taken using a Bomem FT-IR spectrophotometer in the range 2500–4000 cm⁻¹. The samples, about 200 μ m thick, were dried at 90 °C in a vacuum oven overnight before the spectrum was taken. The sample thickness was measured using an electronic micrometer. The deuterated spectrum was subtracted from the sample spectrum of the same material. The difference spectrum was then computer-fitted using Gaussian bands (which were found to give the best fit).¹⁹ A typical difference spectrum and its fitting is shown in Figure 2. A band centered at around 3290 cm⁻¹ is from the O–H stretching vibration of the carboxyl ends and a broad band centered at about 3540 cm⁻¹ is assigned to the O–H stretching vibration of the hydroxyl ends. The integrated absorbances of the hydroxyl and carboxyl ends were then obtained and the end-group concentrations, as well as number average molecular weight, of the samples were calculated using eqs 2–4.

Water Sorption Measurements. The equilibrium water sorption isotherms at 25, 35, and 45 °C were measured for the above samples. Different relative humidities were obtained by using sulphuric acid–water solutions.²⁰ The film samples, about 2 g of each material, were thoroughly dried in a vacuum oven and weighed (“dry” weight) using a Mettler AE240 electronic balance (to 0.01 mg). They were then hung above the solution in a sealed glass jar and left in a temperature-controlled oven. It was found that 3–4 days was enough

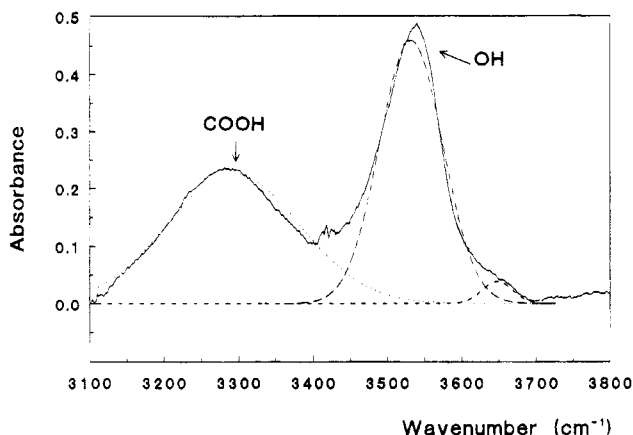


Figure 2. Difference FT-IR spectra of the hydroxyl ends (absorbance centered at 3540 cm^{-1}) and the carboxyl ends (absorbance centered at 3290 cm^{-1}) and the curve fitting using Gaussian bands.

for the equilibrium at various relative humidities to be reached. On removal, the samples were blotted and reweighed ("wet" weight), the difference between the "dry" and "wet" weights giving the equilibrium water content.

Water vapor permeabilities of these material at 25, 35, and $45\text{ }^{\circ}\text{C}$ and 100% relative humidity were also measured using a digital water vapor transmission rate meter. The details of this measurement can be found elsewhere.²¹

The equilibrium water content in the polymers at 100% relative humidity at high temperatures up to $170\text{ }^{\circ}\text{C}$ was measured using a special technique. The main problem with the measurement of water sorption content at high temperatures was that, due to a high diffusion rate at high temperature and a large difference in concentration of water inside and outside the polymer, in the process of the polymer cooling down to room temperature and being exposed to air when weighing, water vapor absorbed into the polymers at high temperature would diffuse out and evaporate very quickly. The water content measured afterward would then be less than it should be. If the sample can be cooled down very quickly while being maintained in water, however, most of the water absorbed into the polymer at high temperature will be retained. This is due to the fact that a large concentration outside the polymer will greatly reduce the chance of the desorption during the cooling process. The desorption at room temperature was found to be very slow and did not affect the measurements.

For these measurements small stainless steel bombs were specifically designed. They had a volume of 80 mL and thin walls which permitted rapid heating and cooling. Valves were fitted to the bomb to discharge air trapped inside and also to release the pressure to permit fast cooling. More importantly, while the bomb was cooling, a pipe connected to the valve sucked cold water into the bomb to keep the samples immersed in water.

The bombs, containing about 10 mL of water, were preheated on a temperature-controlled dry block. After the samples were loaded above the water surface the bombs were closed and air was discharged during heating so that a steam temperature-pressure equilibrium inside the bomb was established. After a predetermined time, the bombs were quenched in cold water with one valve open to release the pressure and the bomb temperature dropped to room temperature in a few seconds. Cold water was sucked into bombs through the valve by the vacuum created inside the bombs during cooling. The samples therefore remained immersed in the water. The samples were dried superficially and weighed as in the isothermal measurements.

Results

The end-group IR absorbances of the samples hydrolyzed at $120\text{ }^{\circ}\text{C}$ are shown in Figure 3, and differences in end-group IR absorption at different hydrolysis times can be seen. Figure 3a shows the spectra of the

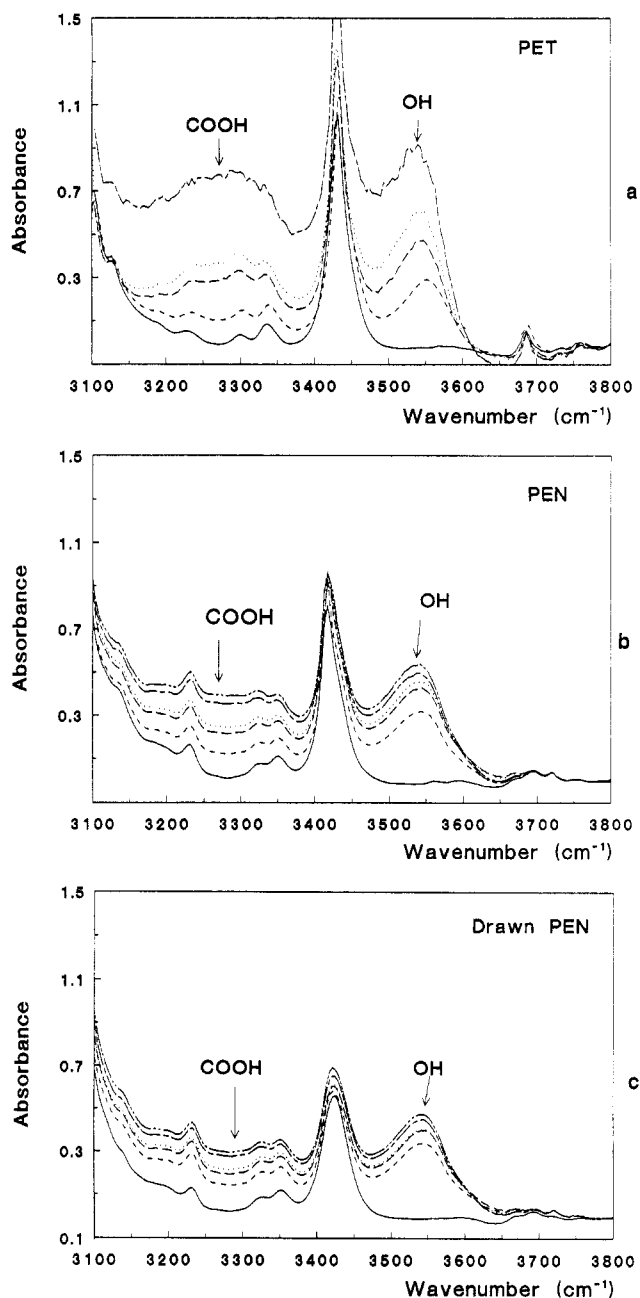
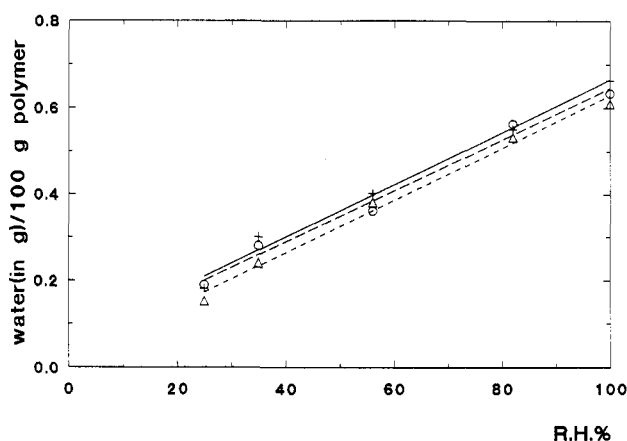


Figure 3. FT-IR spectra in the range $4000\text{--}3000\text{ cm}^{-1}$ of the PEN and PET films samples hydrolyzed for various times at $120\text{ }^{\circ}\text{C}$ in saturated steam: (a) annealed PET, (b) annealed PEN, and (c) drawn and annealed PEN. The deuterated spectrum for each material, in which the absorbances of the hydroxyl and carboxyl ends were removed, is seen at the bottom of each figure as the solid line. Key: (---) original sample, (—) hydrolyzed for 2 days, (... ..) hydrolyzed for 3 days, (— · —) hydrolyzed for 5 days, and (— · · —) hydrolyzed for 6 days.

annealed PET samples hydrolyzed at various times; Figure 3b shows the annealed PEN and Figure 3c shows the drawn and annealed PEN. The deuterated spectra of the PET and PEN which give zero absorbance of hydroxyl ends and carboxyl ends are included in each figure (solid line in the figures) in order to locate the position of the end group absorption band. The absorption band of the carboxyl is seen centered at about 3290 cm^{-1} and the hydroxyl end absorption at about 3540 cm^{-1} . From the increase of the absorbances of the end groups it can be seen that annealed PET is hydrolyzed much faster than PEN. The drawing of PEN had a noticeable effect on the hydrolytic degradation behavior, as seen from comparison between parts b and c of Figure

Table 2. Change in the Concentration of Hydroxyl Ends ([OH]) and Carboxyl Ends ([COOH]), in mol/10⁶ g equiv and Number-Average Molecular Weight (M_n) of the Polyester Samples with Hydrolysis Time at 120, 140, and 160 °C in Saturated Water Vapor^a

hydrolysis temp/°C	hydrolysis time/hours	annealed PET			annealed PEN			drawn and annealed PEN		
		[OH]	[COOH]	M_n	[OH]	[COOH]	M_n	[OH]	[COOH]	M_n
	original sample	89	49	14400	11	38	13400	106	29	14900
120	9	114	67	11100	121	45	12100	111	30	14200
	48	158	123	7100	142	55	10100	118	32	13300
	72	201	150	5700	148	65	9400	122	34	12800
	120	259	215	4200				127	41	12300
	144				154	87	8300	129	43	11900
140	168				165	95	7700	132	46	11500
	10	127	109	8500	161	60	9100	120	33	13100
	14	185	136	6200	166	67	8600	130	36	12100
	24	237	177	4800	180	93	7300	135	43	11200
	38				217	122	5900	143	53	10300
160	48	342	223	3500	270	143	4800	152	56	9600
	64							184	92	7200
	2	117	88	9800	126	64	10600	123	45	11900
	4	177	130	6500	139	74	9400	128	50	11200
	6	237	173	4900	160	91	8000	132	54	10700
	7	279	183	4300	171	101	7400	142	57	10100
	8	289	192	4200	211	104	6300	165	58	9000

^a The values are based on FT-IR analysis.**Figure 4.** Water vapor sorption isotherms at 25 °C for the annealed PET, annealed PEN, and drawn and annealed PEN: (+) PET; (Δ) PEN, and (O) drawn PEN.

3. The drawn samples hydrolyzed much more slowly than the isotropic ones. The hydrolytic degradation was accelerated rapidly by increased temperature for both the PET and the PEN samples. As an example, the PET samples became rather brittle and difficult to handle after 120 h of hydrolytic degradation at 120 °C, but at 160 °C this stage was reached after only about 8 h. PEN samples survived much longer than PET and the drawn PEN was the most resistant to the hydrolytic degradation across the whole temperature range investigated. The concentrations of the end groups and the corresponding number average molecular weights for the samples hydrolyzed at 120, 140, and 160 °C for various times were calculated. These results are summarized in Table 2.

Water vapor sorption isotherms of the materials at 25 °C are shown in Figure 4. The isotherms at 35 and 45 °C (not shown) had very similar characteristics. The isotherms of both PET and PEN can be represented by an almost linear function of vapor pressure and be interpreted in terms of Henry's law. This behavior is typical of strong hydrophobic polymers where the interaction of the water vapour with the polymer is very weak and the water vapor transport behavior is similar to other simple gases.²² Similar results for PET have been reported by other workers.^{23–26}

The solubilities of PET and PEN samples are calculated from the best fit of the isotherms and expressed

either in equilibrium water content (in weight) per 100 g of polymer per unit relative humidity or in the standard unit used for gas solubility as (vapor volume at standard temperature and pressure/(polymer volume) per unit vapor pressure in Pa. These are listed in Table 3, in which the water vapor permeabilities measured using a water vapor transmission rate meter at the same temperatures are also listed. Because the sorption behavior of these polymers obey Henry's law, the permeability (P), the solubility (S), and the diffusion coefficient (D) are related by

$$P = DS \quad (5)$$

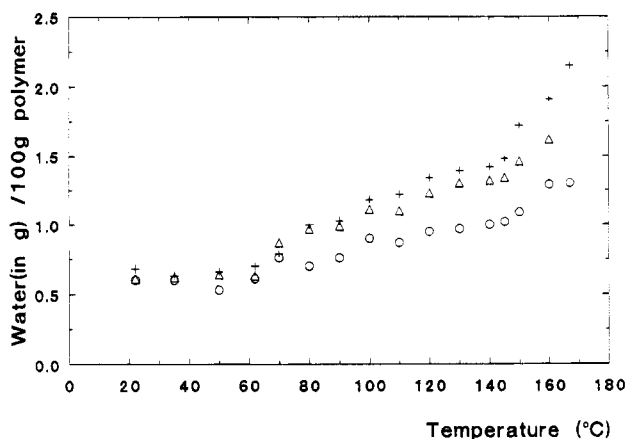
from which the diffusion coefficient, D , can be calculated. The diffusion coefficients of the three samples are again listed in Table 3.

The solubilities of water vapor in PET and PEN samples are similar in the temperature range 25–45 °C. The difference in the permeability and therefore in the diffusion coefficient, however, is rather obvious. The diffusion coefficient of water in PEN is approximately one-third that of PET and drawn PEN has even lower values. Studies by Light and Seymour²⁷ on PET/PEN systems showed very similar results. They had suggested that the reduced segmental mobility due to the naphthalene unit contributes mainly to the reduction of the diffusion coefficient.

The equilibrium water contents at 100% relative humidity at various temperatures up to 170 °C for the PET and PEN samples are shown in Figure 5. The equilibrium water sorption of these samples is seen to increase with temperature, especially at temperatures higher than 100 °C. The increase, however, is different for different materials. PET had the highest water content with a value of 1.9% at 160 °C and drawn PEN had the lowest, 1.3% at the same temperature. Both absorbed about 0.6% at 25 °C. The temperature dependence of equilibrium water content is not a general phenomenon in polymers, but some polymers, e.g. polyarylate²⁸ and polycarbonate,²⁹ have been reported to show temperature dependent water vapor sorptivity. The formation of aqueous microcavities, which were observed by the naked eye during cooling, was suggested to be partly responsible for the temperature dependence of water sorptivities for polycarbonates. However, the PEN and PET samples were carefully examined using

Table 3. Water Vapour Solubilities, *S*, from the Linear Fit of the Isotherms of PET and PEN Samples; Permeability, *P*, from the Water Vapor Transmission Rate Measurements; and the Diffusion Coefficients, *D*, Estimated from $D = P/S$, at 25, 35, and 45 °C

material	temp/°C	saturated vapor pressure at this temp/KPa	<i>S</i> /(wt water/wt polymer)%/RH%	<i>S</i> /(cm ³ (STP)/cm ³ /Pa)	<i>P</i> × 10 ¹³ /[cm ³ (STP)cm/(cm ² s Pa)]	estimated <i>D</i> × 10 ⁹ /(cm ² /s)
ann. PET	25	2.645	0.0068	0.00478	134	2.79
	35	5.627	0.0063	0.00194	136	7.03
	45	12.34	0.0066	0.00092	139	15.0
ann. PEN	25	2.645	0.0061	0.00389	35	0.91
	35	5.627	0.0062	0.00186	40	2.14
	45	12.34	0.0064	0.00087	45	5.19
drawn and ann. PEN	25	2.645	0.006	0.00383	31	0.81
	35	5.627	0.006	0.00180	34	1.90
	45	12.34	0.0057	0.00073	38	5.17

**Figure 5.** Equilibrium water content at various temperature and 100% relative humidity. (+) PET, (Δ) PEN, and (○) drawn PEN.

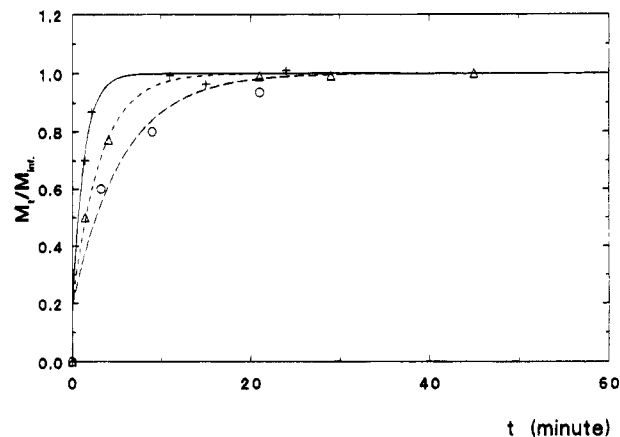
microscopy after the sorption experiments, and voids or cracks in the samples were not found. Repeated measurements on the same samples were in good agreement.

The diffusion coefficients at high temperatures were estimated from the sorption data assuming that diffusion at high temperatures remains concentration independent. For the situation of $M_t/M_\infty \geq 0.55$, Fickian diffusion can be expressed as

$$\frac{M_t}{M_\infty} = 1 - \frac{8}{\pi^2} \exp\left(-\frac{\pi^2 D t}{l^2}\right) \quad (6)$$

where M_t is the water content measured at time t , M_∞ the equilibrium water content, D the diffusion coefficient, and l the thickness of the film sample. The error in using eq 6 for estimation of D is less than 1%.³⁰ The Fickian plot for the PET and PEN samples at 120 °C using eq 6 is shown in Figure 6. The water vapor diffusion coefficients of the PEN and PET samples were estimated from such plots and are listed in Table 4 for two temperatures, 100 and 120 °C. Compared with the estimated diffusion coefficients at low temperatures (25–45 °C) in Table 3, the values at high temperatures showed a much stronger temperature dependence (this can also be seen by Arrhenius plots at different temperature ranges). The difference in diffusion coefficients of different samples is again obvious. PET had the highest water vapor diffusion rate and drawn PEN had the lowest. The diffusion “half time”, $t_{1/2}$, defined by $M_t/M_\infty = 1/2$, is calculated as

$$t_{1/2} = 0.0491 \frac{l^2}{D} \quad (7)$$

**Figure 6.** Fickian plot of the water sorption at 120 °C of isotropic PET, PEN, and drawn PEN: (+) PET, (Δ) PEN, and (○) drawn PEN. The lines seen in the figure are the best fits using eq 6.**Table 4. The Estimated Water Vapor Diffusion Coefficients, *D*, in cm²/s, and Diffusion Half Time, $t_{1/2}$, in min, for PEN and PET Samples from the Sorption Data Measured in Saturated Steam^a**

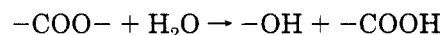
temp/°C	annealed PET		annealed PEN		drawn and annealed PEN	
	<i>D</i> × 10 ⁹	$t_{1/2}$	<i>D</i> × 10 ⁹	$t_{1/2}$	<i>D</i> × 10 ⁹	$t_{1/2}$
100	30	3	8	10	5	16
120	130	0.6	54	2	30	3

^a The sample thickness used in the half-time calculation is 0.02 cm.

and the values are again listed in Table 4, using the film thickness 0.02 cm.

Discussion

It has been suggested that, in the hydrolytic degradation of PET, the only reaction is the acid-catalyzed hydrolysis of the ester linkage:



The back reaction can be neglected in the case of hydrolysis by saturated steam.⁶ Ravens and Ward⁶ showed, by taking PET samples covering a range of initial carboxyl end group concentration of 8–97 mol/10⁶ g equiv, that the rate of hydrolytic degradation of the PET can be expressed by

$$\frac{d[\text{COOH}]}{dt} \propto [\text{EL}][\text{H}_2\text{O}][\text{COOH}]^{1/2} \quad (8)$$

where [EL] is the concentration of ester linkages of the polymer and [H₂O] the concentration of water molecules absorbed inside the polymer. The square root term of

Table 5. Equilibrium Water Content in the Samples in Saturated Steam (100% RH) from Sorption Measurements at the Hydrolysis Temperatures

temp/°C	water steam pressure/kPa	wt of water/wt of polymer, %		
		annealed PET	annealed PEN	drawn and annealed PEN
120	198	1.34 ± 0.03	1.23 ± 0.03	0.95 ± 0.03
140	361	1.42 ± 0.05	1.32 ± 0.05	1.03 ± 0.05
160	618	1.91 ± 0.05	1.63 ± 0.05	1.29 ± 0.05

the carboxyl end group concentration, $[\text{COOH}]^{1/2}$, arises from the autocatalytic function of the carboxyl end group to the hydrolytic degradation due to its weak acidic nature and this hydrolysis was termed as a half-order autocatalytic reaction.⁸

The concentration of ester linkages in PET and PEN can be estimated as follows. For linear polymers, the concentration of ester linkages is reduced as the carboxyl ends increase during hydrolytic degradation. However, because the change in concentration of the ester linkages is very small compared with the initial value, $[\text{EL}]_0$, as a first approximation we have

$$[\text{EL}]_t = [\text{EL}]_0 - [\text{COOH}]_t \approx [\text{EL}]_0 \quad (9)$$

For PET, the concentration of the ester linkages is

$$[\text{EL}]_t \approx [\text{EL}]_0 = 2 \times 10^6 / 192 = 10417 \text{ mol}/10^6 \text{ g equiv}$$

and for PEN it is

$$[\text{EL}]_t \approx [\text{EL}]_0 = 2 \times 10^6 / 242 = 8265 \text{ mol}/10^6 \text{ g equiv}$$

The concentration of water molecules in the polymer does not vary with time in the saturated water steam and can be calculated from the values listed in Table 5 for 120, 140, and 160 °C. Assuming that water only penetrates the amorphous fraction, the possibly affected ester linkage concentration therefore is only $(1 - \text{crystallinity})[\text{EL}]_0$. The water concentration, however, is increased to $[\text{H}_2\text{O}]/(1 - \text{crystallinity})$ if all the water molecules are confined to the amorphous region. Furthermore, our infrared end-group analysis suggested that all the polymer chain ends are in the amorphous region.¹⁹ The effective end group concentration in eq 8 is then increased to $[\text{COOH}]/(1 - \text{crystallinity})$. Note that the crystallinity here refers to the original crystallinity of the samples. The effect of hydrolysis on sample crystallinity^{13–15} is irrelevant to our consideration here. Taking all these factors into consideration, eq 8 can be written as

$$\frac{d[\text{COOH}]}{dt} = \frac{k}{(1 - \text{crystallinity})^{1/2}} [\text{EL}][\text{H}_2\text{O}][\text{COOH}]^{1/2} = K[\text{COOH}]^{1/2} \quad (10)$$

where k is the "true" chemical reaction constant and

$$K = \frac{k}{(1 - \text{crystallinity})^{1/2}} [\text{EL}][\text{H}_2\text{O}] \quad (11)$$

is the "apparent" reaction constant. Equation 10 can

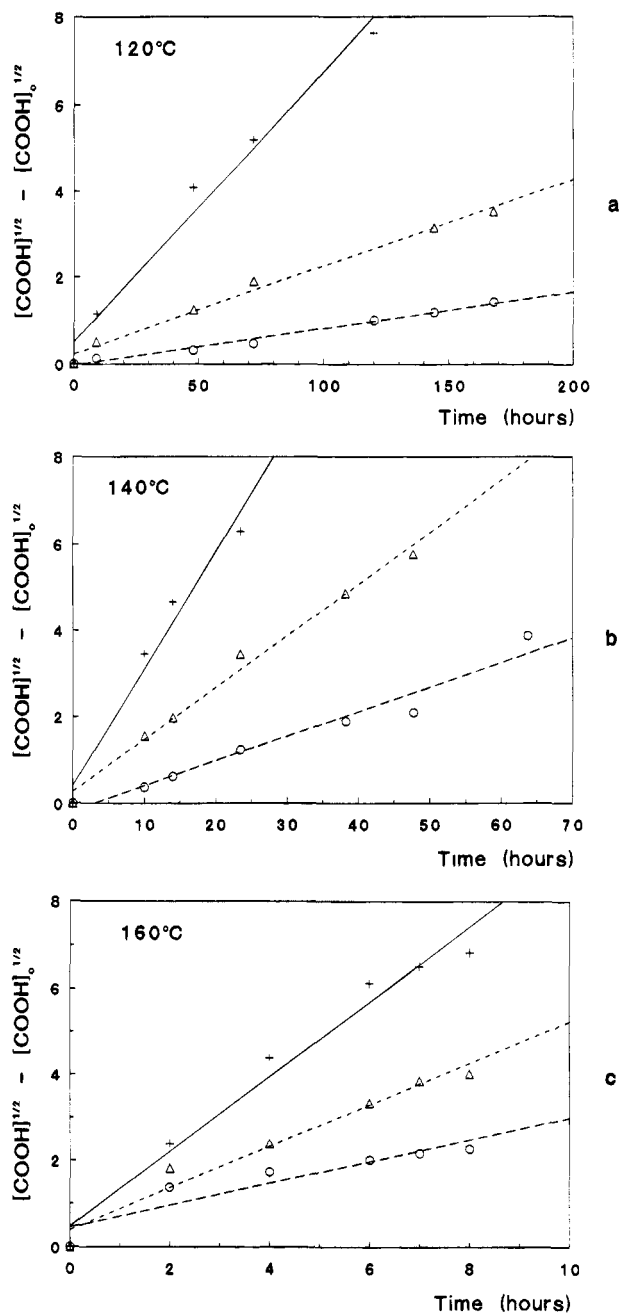


Figure 7. Plots of the half-order autocatalytic reaction rates of annealed PET, annealed PEN, and drawn and annealed PEN film samples hydrolyzed in saturated steam for various times. Samples hydrolyzed at (a) 120 °C, (b) 140 °C, and (c) 160 °C: (+) PET, (Δ) PEN, and (O) drawn PEN.

then be integrated with time, which gives

$$[\text{COOH}]_t^{1/2} - [\text{COOH}]_0^{1/2} = \frac{K}{2}t \quad (12)$$

where $[\text{COOH}]_t$ is the concentration of the carboxyl ends at time t and $[\text{COOH}]_0$ is the initial concentration.

The plots of $[\text{COOH}]_t^{1/2}$ as a function of time for the hydrolysis of PET and PEN samples are shown in Figure 7a, 7b, and 7c, for 120, 140, and 160 °C, respectively. The "apparent" half-order reaction rate constant, K , obtained as the slope of the best linear fit in the figures, is an overall indication of how fast the polymer would degrade in the hydrolysis reaction. These values are listed in Table 6. The higher the value, the faster the hydrolytic degradation of the sample. The hydrolytic degradation rate can also be expressed by the hydrolytic degradation half time, $t_{1/2}$,

Table 6. "Apparent" Chemical Reaction Rate Constant, K , and the Hydrolysis Reaction Half-Life Time, $t_{1/2}$, of PET and PEN Samples, Derived from the Half-Order Autocatalytic Reaction Mechanism

hydrolysis temp/°C	annealed PET		annealed PEN		drawn and annealed PEN	
	K	$t_{1/2}/h$	K	$t_{1/2}/h$	K	$t_{1/2}/h$
120	0.125	46	0.041	127	0.017	265
140	0.56	11	0.24	22	0.12	39
160	1.74	3	0.97	5	0.50	9
apparent activation energy/kJ mole ⁻¹	94 ± 5		113 ± 6		117 ± 5	

defined as the time for the concentration of carboxyl ends to increase during hydrolytic degradation to a value twice its original value. From eq 12, it follows that

$$t_{1/2} = \frac{0.414[\text{COOH}]_0^{1/2}}{(K/2)} \quad (13)$$

These $t_{1/2}$ values are also listed in Table 6.

Table 6 shows the difference in the hydrolytic degradation rate in saturated steam for different samples. From these results, PEN, especially in the drawn state, would be expected to have a much longer service life than PET. The lower concentration of the ester linkages in PEN and the lower water sorption content of PEN, especially drawn PEN, contributes greatly to the lower values of the "apparent" hydrolytic degradation rate and longer life, as shown in eq 11. However, the "true" chemical reaction rates, k , of PEN samples, listed in Table 7, are still seen to be lower than those of PET. The difference between the oriented PEN sample and isotropic samples is again apparent.

An important issue in studying the hydrolytic stability of polymers is to find which factor, diffusion or chemical reaction, dominates the hydrolytic degradation. A way to determine whether the degradation is diffusion rate controlled or chemical reaction rate controlled is to compare diffusion rates with the chemical degradation rate. The diffusion rate is generally characterized by the diffusion half time, $t_{1/2}$, as defined in eq 7. The chemical reaction rate for polyester hydrolytic degradation can be illustrated by either the time required to double the carboxyl end group concentration, as in eq 13, or by the time required for the molecular weight of the polymer to drop to half of its original value. Table 8 gives such a comparison using data seen in Tables 2, 4, and 6. The sample thickness used for all calculations was 0.2 mm.

The comparison in Table 8 shows that the diffusion half time is on the order of minutes while the chemical reaction half time is on the order of 100 h. A similar conclusion was reported for crystalline PET by Davies et al.⁷ The difference between the water vapor diffusion rates and the hydrolytic degradation rates is so large that errors in the estimation of the diffusion coefficients

would not alter this significantly. It is then concluded that, since the water vapor transport rate far exceeds that required to hydrolyze the polymer chains, the hydrolytic degradation of both PET and PEN at high temperatures is chemical reaction rate determined. The difference in diffusion rates between the PEN and PET is not the reason for the better hydrolytic stability of PEN.

The difference in molecular chain packing between PET and PEN may be a reason for the difference in their hydrolytic degradation rates. Campanelli et al.³¹ studied the hydrolytic degradation rates of PET in the melt state and, using the Arrhenius equation, extrapolated the reaction rate constants to low temperatures. They found that the extrapolated values were orders of magnitude higher than the experimental values obtained at low temperatures. The molecular chain packing in the solid state was believed to have an obvious impact on the reduction of the hydrolytic degradation rate in the solid state. In our case, the naphthalene rings in the molecular chain produce a more extended chain configuration than that of PET.² Drawing enhances this orientation and makes it more extended. Such configurations result in smaller dielectric constants.^{32,33} These might contribute to a lower dissociation constant for water molecules which have penetrated into the polymer and for the carboxyl ends to create a weak acid, which would reduce the chemical reaction rate.³⁴

The temperature dependence of the hydrolysis reaction rate in the temperature range of 120–160 °C was found to follow the Arrhenius relationship for the chemical reaction constant:

$$K = K_0 e^{-E/RT} \quad (14)$$

where E is the activation energy of the hydrolytic reaction, R the gas constant, and T the absolute temperature. The plots of $\ln K$ vs $1/T$, shown in Figure 8, resulted in straight lines, and the slopes of the lines give the activation energies which are again listed in Table 6. The apparent activation energy of 25 ± 1 kcal/mol or 94 ± 5 kJ/mol for the annealed PET, obtained from this study, compares with a published value of 26.9 kcal/mol for a PET sample with 50% crystallinity hydrolyzed at a similar temperature.⁷ The "true" chemical reaction activation energy, obtained by using the "true" chemical reaction rate constants, are listed in Table 7. The activation energy of the "true" chemical reaction of PEN is apparently greater than that of PET.

Conclusions

Semicrystalline unoriented PEN films exhibit better resistance to hydrolytic degradation in saturated steam at temperatures in the range 120–160 °C than semicrystalline unoriented PET films. A semicrystalline oriented PEN film exhibits still better resistance to hydrolytic degradation. Water vapor diffusion rates and water vapor sorptivity are lower in PEN, especially

Table 7. "True" Chemical Reaction Rate Constants of PET and PENs Hydrolyzed at 120–160 °C^a

hydrolysis temp/°C	annealed PET	annealed PEN	drawn and annealed PEN
120	$(1.2 \pm 0.1) \times 10^{-8}$	$(0.6 \pm 0.1) \times 10^{-8}$	$(0.23 \pm 0.05) \times 10^{-8}$
140	$(3.5 \pm 0.3) \times 10^{-8}$	$(2.1 \pm 0.2) \times 10^{-8}$	$(1.2 \pm 0.1) \times 10^{-8}$
160	$(10.2 \pm 0.9) \times 10^{-8}$	$(7.9 \pm 0.8) \times 10^{-8}$	$(5.0 \pm 0.3) \times 10^{-8}$
activation energy/kJ·mole ⁻¹	75 ± 5	92 ± 7	109 ± 6

^a The contributions of the concentration of ester linkages, the water contents, and the crystallinity of the polymer to the hydrolysis resistance have been excluded. A half-order autocatalytic reaction mechanism is used.

Table 8. Comparison between the Diffusion Rate and the Hydrolysis Reaction Rate^a

sample	diffusion half time ($t_{1/2}$) from eq 2/min	time to double carboxyl end group concentration/h	time to reduce the number average molecular weight by half/h
ann. PET	0.6	30	50
ann. PEN	2	120	200
drawn and ann. PEN	3	200	300

^a All the data are obtained from the measurements at 120 °C in saturated steam.

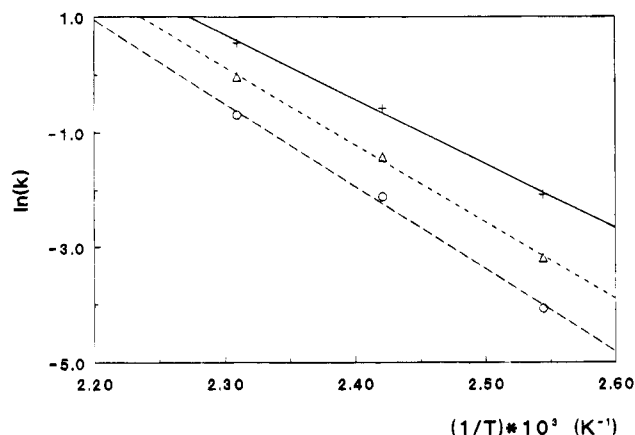


Figure 8. Temperature dependence of the hydrolysis reaction rate constants in the range 120–160 °C. The “true” chemical reaction rate constants are those excluding the contributions from the effect of concentration of the ester linkages and the water contents absorbed during the hydrolysis: (+) PET, (Δ) PEN, and (O) drawn PEN.

oriented PEN, than they are in PET. In all these cases, however, the water vapor diffusion rates exceed the experimentally measured rates of hydrolytic degradation by 3–4 orders of magnitude. The hydrolysis reaction is therefore not water diffusion rate controlled but chemical reaction rate controlled, and the reaction rate is best described by a half-order autocatalytic reaction. The lower water absorption and lower ester linkage concentration in PEN contribute to the improved hydrolytic stability compared to PET. The “true” chemical reaction rates, however, calculated from the half-order autocatalytic reaction mechanism for the hydrolysis in saturated steam, still showed the following rates: semicrystalline PET > semicrystalline PEN > oriented semicrystalline PEN, with a factor 2–3 between the PET and the PEN samples.

Acknowledgment. The authors wish to thank the SERC and SCAPA Group Plc for supporting the project. The supply of PEN cast films by AMOCO Chemicals (Europe) SA, Geneva, Switzerland, and of PEN and PET films by ICI Films, Middlesborough, UK, is greatly

appreciated. We thank Professor J. E. McIntyre in particular for his many valuable suggestions during the course of the work. We are grateful to Mr. P. L. Carr for helpful discussions about this paper and Mr. G. P. Thompson for excellent technical help.

References and Notes

- (1) Mencik, Z. *Chem. Prumysl.* **1967**, 17, 78.
- (2) Quchi, T.; Nasai, M.; Shimotsumas, S. *J. Appl. Polym. Sci.* **1977**, 21, 3445.
- (3) Buchner, S.; Wiswe, D.; Zachmann, H. G. *Polymer* **1989**, 30, 480.
- (4) Ghaheem, A. M.; Porter, R. S. *J. Polym. Sci., Polym. Phys. Ed.* **1989**, 27, 2587.
- (5) *Res. Disclosure* **1988**, 294, 1714.
- (6) Ravens, D. A. S.; Ward, I. M. *Trans. Faraday Soc.* **1961**, 57, 150.
- (7) Davies, T.; Goldsmith, P. L.; Ravens, D. A. S.; Ward, I. M. *J. Phys. Chem.* **1962**, 66, 175.
- (8) Ravens, D. A. S.; Sisley, J. E. Chapter in *Chemical Reaction of Polymers*; Fettes, E. M., Ed.; Interscience Publishers: New York, 1964.
- (9) Zimmermann, H.; Kim, N. T. *Polym. Eng. Sci.* **1980**, 20, 680.
- (10) Brown, D. W.; Lowry, R. E.; Smith, L. S. *Macromolecules* **1980**, 13, 248.
- (11) Allen, N. S.; Edge, M.; Mohammadian, M. *Eur. Polym. J.* **1991**, 27, 1373.
- (12) Allen, N. S.; Edge, M.; Mohammadian, M.; Jones, K. *Polym. Degrad. Stabl.* **1994**, 43, 229.
- (13) Cagiao, M. E.; Balta-Calleja, F. J.; Vanderdonckt, C.; Zachmann, H. G. *Polymer* **1993**, 34, 2024.
- (14) Balta-Calleja, F. J.; Cagiao, M. E.; Zachmann, H. G.; Vanderdonckt, C. *J. Macromol. Sci. Polym. Phys. Ed.* **1994**, 33, 333.
- (15) Miyagi, A.; Wunderlich, B. *J. Polym. Sci.: Polym. Phys. Ed.* **1972**, 10, 2073.
- (16) Fakirov, S.; Fischer, E. W.; Schmidt, G. F. *Makromol. Chem.* **1975**, 176, 2459.
- (17) Lide, D. R., Ed. *Handbook of Chemistry and Physics*, 73rd ed.; CRC Press: Boca Raton, 1993.
- (18) Ward, I. M. *Trans. Faraday Soc.* **1957**, 53, 1406.
- (19) Zhang, H.; Rankin, A.; Ward, I. M. *Polymer*, in press.
- (20) *Annual Book of ASTM Standard*, E 104–8S, Standard Practice for Maintain Constant Relative Humidity by Means of Aqueous Solution, 1992.
- (21) Orchard, G. A. J.; Spiby, P.; Ward, I. M. *J. Polym. Sci., B: Polym. Phys.* **1990**, 28, 603.
- (22) van Krevelen, D. W. *Properties of Polymers*, Elsevier: Amsterdam and London, 1990.
- (23) Jabarin, S. A.; Lofgren, E. A. *Polym. Eng. Sci.* **1986**, 26, 620.
- (24) Langevin, D.; Grenet, J.; Saiter, J. M. *Eur. Polym. J.* **1994**, 30, 339.
- (25) Yasuda, H.; Stannett, V. J. *Polym. Sci.* **1962**, 57, 907.
- (26) Hubbell, W. H.; Brandt, H.; Munir, Z. A. *J. Polym. Sci.: Polym. Phys. Ed.* **1975**, 13, 493.
- (27) Light, R. R.; Seymour, R. W. *Polym. Eng. Sci.* **1982**, 22, 857.
- (28) Golovoy, A.; Cheng, M. F. *J. Appl. Polym. Sci.* **1988**, 35, 1511.
- (29) Golovoy, A.; Zinbo, M. *Polym. Eng. Sci.* **1989**, 28, 1733.
- (30) Vergnaud, J. M., *Liquid Transport Process in Polymeric Materials*, Prentice Hall: New Jersey, 1991, p 4ff.
- (31) Campanelli, J. R.; Kamal, M. R.; Cooper, D. G. *J. Appl. Polym. Sci.* **1993**, 48, 443.
- (32) Maxwell, A. S., private communication.
- (33) Ezquerro, T. A.; Balta-Calleja, F. J.; Zachmann, H. G. *Acta Polym.* **1993**, 44, 18.
- (34) Atkins, P. W. *Physical Chemistry*, Oxford University Press: Oxford, 1978; Chapter 26.

MA9507709